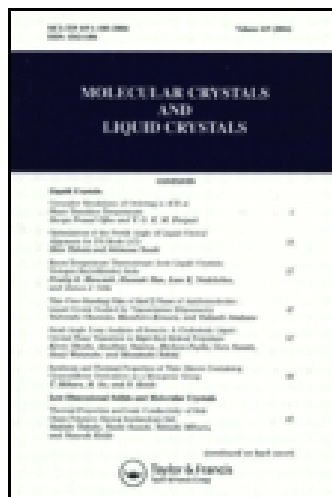


This article was downloaded by: [Australian National University]
On: 01 January 2015, At: 22:31
Publisher: Taylor & Francis
Informa Ltd Registered in England and Wales Registered Number: 1072954
Registered office: Mortimer House, 37-41 Mortimer Street, London W1T 3JH,
UK



Molecular Crystals and Liquid Crystals

Publication details, including instructions for authors and subscription information:

<http://www.tandfonline.com/loi/gmcl20>

Synthesis, Characterization, and Dilatometric Studies on N-(p-n-Alkoxybenzylidene)-p-n-pentyloxyanilines Compounds

N. Ajeetha^a, V. G. K. M. Pisipati^a, M. Ramakrishna Nanchara Rao^b & P. V. Datta Prasad^c

^a Centre for Liquid Crystal Research and Education, Faculty of Physical Sciences, Acharya Nagarjuna University, Nagarjunanagar, India

^b Department of Physics, A. J. Kalasala, Machilipatnam, India

^c Department of Physics, Hindu College, Machilipatnam, India

Published online: 31 Jan 2007.

To cite this article: N. Ajeetha, V. G. K. M. Pisipati, M. Ramakrishna Nanchara Rao & P. V. Datta Prasad (2006) Synthesis, Characterization, and Dilatometric Studies on N-(p-n-Alkoxybenzylidene)-p-n-pentyloxyanilines Compounds, *Molecular Crystals and Liquid Crystals*, 457:1, 3-25, DOI: [10.1080/15421400500447108](https://doi.org/10.1080/15421400500447108)

To link to this article: <http://dx.doi.org/10.1080/15421400500447108>

PLEASE SCROLL DOWN FOR ARTICLE

Taylor & Francis makes every effort to ensure the accuracy of all the information (the "Content") contained in the publications on our platform. However, Taylor & Francis, our agents, and our licensors make no representations or warranties whatsoever as to the accuracy, completeness, or suitability for any purpose of the Content. Any opinions and views

expressed in this publication are the opinions and views of the authors, and are not the views of or endorsed by Taylor & Francis. The accuracy of the Content should not be relied upon and should be independently verified with primary sources of information. Taylor and Francis shall not be liable for any losses, actions, claims, proceedings, demands, costs, expenses, damages, and other liabilities whatsoever or howsoever caused arising directly or indirectly in connection with, in relation to or arising out of the use of the Content.

This article may be used for research, teaching, and private study purposes. Any substantial or systematic reproduction, redistribution, reselling, loan, sub-licensing, systematic supply, or distribution in any form to anyone is expressly forbidden. Terms & Conditions of access and use can be found at <http://www.tandfonline.com/page/terms-and-conditions>

Synthesis, Characterization, and Dilatometric Studies on N-(*p*-*n*-Alkoxybenzylidene)-*p*-*n*-pentyloxylanilines Compounds

N. Ajeetha

V. G. K. M. Pisipati

Centre for Liquid Crystal Research and Education, Faculty of Physical Sciences, Acharya Nagarjuna University, Nagarjunanagar, India

M. Ramakrishna Nanchara Rao

Department of Physics, A. J. Kalasala, Machilipatnam, India

P. V. Datta Prasad

Department of Physics, Hindu College, Machilipatnam, India

*Synthesis, textural characterization, differential scanning calorimetry, and dilatometry studies are carried out on a new homologous series of N-(*p*-*n*-alkoxy benzylidene)-*p*-*n*-pentyloxy anilines (*nO.O5*) where $n = 1-18$. The lower homologues of this series ($n = 1-5$) and a higher homologue ($n = 16$) exhibit monotropic Liquid Crystal (LC) phase. The other members of the series show enantiotropic LC phases, while 18O.O5 is a nonliquid crystal. The dilatometric studies on 7O.O5, 10O.O5, 13O.O5 and 16O.O5 reveal the first-order nature of Isotropic to Nematic Phase (IN), Isotropic to Smectic A Phase (IA), Nematic to Smectic C Phase (NC), Smectic A to Smectic B Phase (AB), Smectic C to Smectic B Phase (CB), and Smectic A to Krystal Phase (AK) transitions. The pretransition effects are estimated from dilatometry results. The results are compared with the available data on *nO.m* compounds.*

Keywords: dilatometry; liquid crystals; pretransitional effects

INTRODUCTION

The benzylidene aniline Schiff base liquid-crystalline (LC) compounds, N-(*p*-*n*-alkoxybenzylidene)-*p*-*n*-alkylanilines, popularly known as *nO.ms*, exhibit rich but subtle polymesomorphism [1,2]. It is very

Address correspondence to V. G. K. M. Pisipati, Centre for Liquid Crystal Research and Education, Faculty of Physical Sciences, Acharya Nagarjuna University, Nagarjunanagar 522 510, A.P., India. E-mail: venkata_pisipati@hotmail.com

interesting to note that the position of the oxygen atom on either sides of the rigid core ($nO.m$ and $n.Om$) plays a major role in the occurrence of the phase variant and the clearing temperature of the mesogenic compound [3,4]. The recent investigations on similar Schiff bases with $n.Om$ and $nO.Om$ chains revealed that the clearing temperatures are elevated to above 100°C whereas $nO.m$ compounds exhibit a clearing temperature below 100°C [5].

A physical system at a given temperature is completely described by the equilibrium value of the relevant order parameter and the fluctuation effects. During phase transition, the free energy of the system remains continuous, and the thermodynamic quantities such as volume, entropy, and heat capacity undergo discontinuous changes. The dilatometric investigation of thermotropic liquid crystals, to obtain relations between the molecular structure and mesomorphic properties, have been performed using the specific volume ($v = 1/\rho$) and molar volume ($Mv = \text{molecular weight/density } (\rho)$), which are closely related to density. The thermal expansion coefficient ($\alpha = (1/Mv) dMv/dT$) of the material can also be obtained from dilatometry. Dilatometric studies are long known to determine the order of the phase transitions and the associated pretransitional behavior at the transition involving isotropic liquid to the first mesomorphic phase, which infers the molecular interaction and contribution for the growth and stability of the LC phase [6,7].

As a part of our ongoing systematic studies on benzylidene aniline LC compounds, the present article reports the synthesis, characterization, and dilatometric studies on N-(*p-n*-alkoxybenzylidene)-*p-n*-pentoxyanilines, $nO.O5$ compounds. The phase variants, transition temperatures, associated enthalpy values, and nature of the transitions involving isotropic (I), nematic (N), smectic A (S_A), smectic C (S_C), smectic B (S_B), and smectic G (S_G) phases are presented. The pressure dependence of the transition temperatures is estimated from measured volume jumps and the enthalpy data. The results are compared with the data available on $nO.m$ compounds.

EXPERIMENTAL

The compounds are prepared by condensation of the corresponding *p-n*-alkoxybenzaldehyde (0.1 mol) from $n = 1-16$ with pentoxyaniline (0.1 mol) by refluxing the reactants in absolute ethanol in the presence of a few drops of glacial acetic acid. After refluxing the mixture for 4 to 5 h, the solvent is removed by distillation, and the compound is further purified by recrystallization in cold ethanol. The molecular formula for $nO.O5$ compounds is given in Fig. 1. The textural identification and

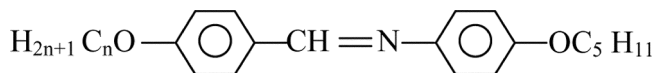


FIGURE 1 General molecular structure of $n\text{O}.05$ compounds.

the phase transition temperatures are determined using a polarizing microscope (Olympus BX 50) supplemented by an optical display (DP-10) at a scan rate of 0.1°C per min. A Perkin-Elmer DSC-7 instrument is used to determine the transition temperatures and the associated enthalpy values.

RESULTS AND DISCUSSION

Characterization of Liquid-Crystalline Phases of N-(*p-n*-alkoxybenzylidene)-*p-n*-pentyloxy anilines ($n\text{O}.05$)

Although the optical textural observations reveal that these compounds exhibit traditional textures, they are found to exhibit interesting phase variants compared to the compounds of N-(*p-n*-alkoxybenzylidene)-*p-n*-pentylanilines ($n\text{O}.5$) [8]. The textural observations of this series of compounds exhibit two monovariant, one divariant, one trivariant, and one quadravariant phase-sequenced systems. The compounds 10.05 to 60.05 exhibit one type of monovariant phase sequence, whereas the higher homologue 160.05 exhibits a qualitative type of monovariant sequence. The middle members of the series exhibit rich polymesomorphism, quadra- (70.05) and tri- (80.05 to 100.05) variant phase sequences. However, the higher homologous series are found to exhibit divariant (110.05 to 140.05) phase sequences.

On cooling from the I phase, these series of compounds with $n = 1-7$ are found to grow a N phase, exhibiting threaded marble texture at $95.2, 119.3, 100.5, 110.9, 109.7, 110.5,$ and 106.5°C respectively. The texture observed in these compounds is similar to those in the $n\text{O}.5$ series of $n\text{O}.m$ compounds that exhibit an N phase [9]. On further cooling, these compounds with $n = 1-6$ are found to condense into solid (crystalline) phase at $83.5, 88.5, 96.2, 109.2, 109.1,$ and 102.5°C respectively. The compounds with $n = 4$ and 5 show very narrow nematic thermal ranges of 1.7 and 0.6°C . Although our earlier report [3] on 50.05 presented it as S_G , our present meticulous and systematic studies on the compound confirmed that the phase is nematic. The error in our earlier report may be attributed to the extremely small thermal range involved with the LC phase. Because, the transition from isotropic to LC phase occurs around $\sim 109^\circ\text{C}$ in the remaining lower homologues

(with $n = 1-6$) that exhibited the nematic phase, it may be readily accepted that the LC phase in 50.O5 is nematic conclusively.

However, on further cooling, the compound 70.O5 was found to exhibit an altogether different texture (from usual marble threaded N texture) consisting of schlieren brushes characteristic of S_C phase occurrence at 95.2°C. This compound is unique in this series as it exhibits a different phase variant than the other compounds. On further cooling of the sample, these schlieren brush texture is found to transform smooth glossy focal conic texture at 89.5°C, characterizing the phase as S_B . Further lowering of temperature leads to a change of focal conic texture into striped broken focal conic fan texture at 86.2°C. A similar trend of phase variance is observed in the case of 70.5, characterizing the phase as S_G [8]. The overall textural observations in this compound, 70.O5, reveals that it is a case of Nematic, Smectic C, Smectic B, Smectic G (NCBG) phase variant.

The remaining compounds in the $nO.O5$ series with $n = 8-11, 13-16$ show a S_A phase in the form of batonnets at 104.6, 105.3, 106.2, 89.1, 104.5, 99.5, and 91.3°C on cooling these samples from isotropic melt. These batonnets that grow in the I phase coalesce to form a clear focal conic fan texture with the further decrease of temperature. This S_A phase is also found to exhibit pseudo-I appearance in the homeotropic aligned region. This observation further confirms the orthogonal structural arrangement of the smectic phase. These observations are similar to those observed in the case of 80.5 and the lower homologues of 130.*m*, 140.*m*, and 160.*m* compounds [10]. These observations in the wake of reports on 80.5, 130.*m*, 140.*m*, and 160.*m* compounds taken together confirm that the phase occurs in $n = 8-11, 13$, and 16 of $nO.O5$ series and is S_A . In the case of compound 160.O5, the cooling of I liquid results in the formation of a solid (crystal) phase at 90.2°C. However, in the case of the rest of the compounds, further lowering of temperature results in the appearance of transient transition bars followed by the appearance of smooth focal conic fans with glossy surfaces at 95.3, 100.3, 104.3, 87.2, 89.4, 91.3, and 88.2°C for compounds 80.O5, 90.O5, 100.O5, 110.O5, 130.O5, 140.O5, and 150.O5 respectively. The appearance of transient transition bars and the formation of smooth focal conic fan texture with reduced discontinuities at boundaries implies that this transformation is from S_A to S_B . However, this occurrence of $S_A S_B$ transitions falls as a common observation because many Schiff-based $nO.m$ compounds show S_A and S_B phases [11].

On further cooling of compounds with $n = 11, 13, 14$, and 15, the S_B focal conic fan texture is found to change to a solid (crystal) sandy appearance at 73.4, 76.2, 78.4, and 81.3°C. The other compounds with

TABLE 1 The Comparative Phase Variant Table of $nO.05$ vs. $nO.5$ Compounds

Compound	1	2	3	4	5	6	7	8	9	10	11	13	14	15	16
$nO.05$	N	N	N	N	N	N	NACG	ABG	ABG	ABG	AB	AB	AB	AB	A
$nO.5$	N	N	NB	NABG	NACFG	NABG	NACBG	ABG	AF						

N-Nematic; NB-Nematic, Smectic B; NABG-Nematic, Smectic A, Smectic B, Smectic G; NACFG-Nematic, Smectic A, Smectic C, Smectic F, Smectic G; NACBG-Nematic, Smectic A, Smectic C, Smectic B, Smectic G; ABG-Smectic A, Smectic B, Smectic G; AB-Smectic A, Smectic B; A-Smectic A; AF-Smectic A, Smectic F.

$n = 8, 9,$ and $10,$ on further cooling of S_B phase, results in the formation of striped broken focal conic fan texture (from smooth focal conic S_B texture) at $60.0, 85.6,$ and 87.4°C respectively. These observations are similar to those observed in the case of 80.5 and other $nO.m$ compounds, indicating the growth of S_G phase. Later, further cooling of the sample results in the transformation of S_G phase to solid (crystal) phase at $73.6, 75.2,$ and 71.2°C in the $nO.O5$ compounds with $n = 8, 9,$ and 10 respectively.

These results imply that these homologous compounds ($nO.O5$) exhibit five types of variants; **N, NCBG** (Nematic, Smectic C, Smectic B, Smectic G), **A, AB, ABG**. This observation stands contrast to those **N, NABG, NB, NACFG, NACBG, ABG,** and **AF** phase variants exhibited by $nO.5$ compounds. This clearly indicates that the introduction of an electronegative oxygen atom on the aniline side of the LC molecule quenches some of the mesomorphic phases and at the same time elevates the clearing temperatures. The present textural observations concur with the results obtained in the case of $nO.m$ compounds. The phase variants exhibited by the $nO.O5$ series and the reported $nO.5$ series are presented in Table 1. The phase diagram of $nO.O5$ compounds is given in Fig. 2.

Table 2 provides information regarding the transition temperatures from Differential Scanning Calorimetry (DSC) and thermal microscopy and the corresponding enthalpy values from DSC at different

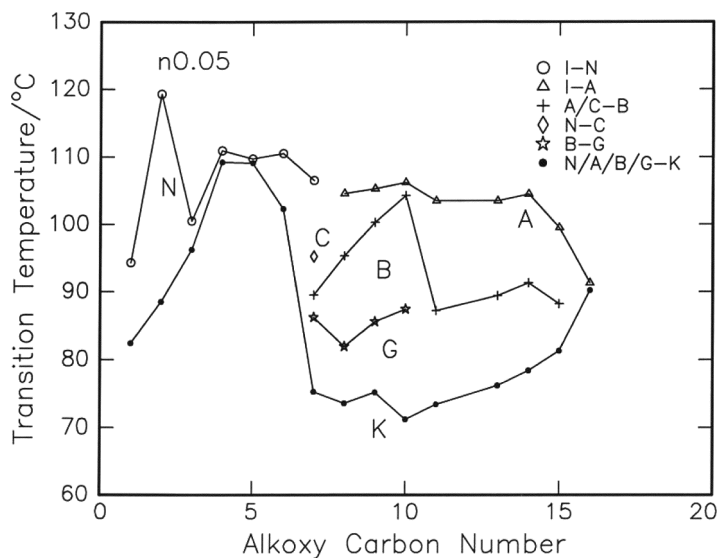


FIGURE 2 Phase diagram of $nO.O5$ compounds.

TABLE 2 Transition Temperatures (in °C) along with Enthalpy Values of Alkoxy Benzylidene Pentyloxy Anilines (nO.05) and the Transition Temperatures (in °C) of Alkoxy Benzylidene Pentyl Aniline (nO.5)

Compound name	Phase variant	Method	Parameter	I-N/A/G	N/A-A/B/C	A-C/B	A/C-F/B	A/B/F-G	I/N/A/G-K	Ref.
10.5	N	TM	Cooling	62.8					39.7	[1]
10.05	N	DSC	Heating $\Delta H/J/gm$						105.23	
			Cooling	92.96					51.44	
			$\Delta H/J/gm$	0.46					80.63	
			Cooling	95.2					45.97	
20.5	N	TM	Cooling	90.4					83.5	
20.0.5	N	DSC	Heating	118.36					63.3	
			$\Delta H/J/gm$	5.77					93.17	[1]
			Cooling	115.53					148.06	
			$\Delta H/J/gm$	6.10					84.58	
30.5	NB	TM	Cooling	119.3					134.30	
30.05	N	DSC	Heating	71.1	23.6				88.5	[1]
			$\Delta H/J/gm$						—	
			Cooling	101.58					105.62	
			$\Delta H/J/gm$	2.52					104.28	
			Cooling	100.5					96.58	
40.5	NABG	TM	Cooling	84.6					83.27	
40.05	N	DSC	Heating		44.4	41.5		30	96.2	[1]
			$\Delta H/J/gm$						28	
			Cooling	110.66					113.60	
			$\Delta H/J/gm$	1.10					140.05	
			Cooling	110.9					108.10	
			$\Delta H/J/gm$						133.00	
			Cooling						109.2	

(Continued)

TABLE 2 Continued

Compound name	Phase variant	Method	Parameter	I-N/A/G	N/A-A/B/C	A-C/B	A/C-F/B	A/B/F-G	I/N/A/G-K	Ref.
50.05	NACFG	TM	Cooling	77.80	54.40	53.10	49.00	47.00	28	[1]
50.05	N	DSC	Heating $\Delta H/J/gm$						113.25 86.09	
			Cooling	108.97 ^a					108.80 ^a	
			$\Delta H/J/gm$						75.98	
60.05	NABG	TM	Cooling	109.7					109.1	
60.05	N	DSC	Heating	85.2	75.2	61.6		45.2	40.0	[1]
			Heating	109.23					101.51	
			$\Delta H/J/gm$	4.07					84.26	
			Cooling	106.11					96.08	
			$\Delta H/J/gm$	4.02					80.65	
70.05	NACBG	TM	Cooling	110.5					102.3	
70.05	NCBG	DSC	Heating	83.2	79.2	68.3	64.4	58.0	23	[15]
			Heating	107.35					96.57	
			$\Delta H/J/gm$	2.88					89.98	
			Cooling	104.64	93.37		88.24 ^a	87.24 ^a	72.48	
			$\Delta H/J/gm$	3.51	8.15				10.51	
80.05	ABG	TM	Cooling	106.5	95.2		89.5	86.2	75.3	
80.05	ABG	DSC	Heating	85.7	70.8			52.7	42.2	[11]
			Heating	108.87	99.65				89.79	
			$\Delta H/J/gm$	4.00	4.24				77.86	
			Cooling	105.85	96.44			83.26	74.74	
			$\Delta H/J/gm$	3.78	3.71			4.23	49.80	
90.05	ABG	TM	Cooling	104.6	95.3			81.9	73.6	
90.05	ABG	DSC	Heating	87.5	74.5			60.0	33.0	[14]
			Heating	101.13	106.30				93.15	
			$\Delta H/J/gm$	3.40	3.92				97.41	

				103.67	98.40	83.46	73.42
		Cooling	$\Delta H/J/gm$	4.06	3.39	3.43	71.60
	TM			105.3	100.3	85.6	75.2
100.5	ABG	Cooling		86.5	73.6	70.3	[1]
100.05	ABG	Heating		106.81 ^a	104.64 ^a	91.18	
		$\Delta H/J/gm$				117.58	
		Cooling		104.39 ^a	102.11 ^a	85.19	
		$\Delta H/J/gm$				7.40	
110.5	ABG	Cooling		106.2	104.3	87.4	
110.05	AB	Cooling		88.2	97.7	50.2	[16]
		Heating		105.87			
		$\Delta H/J/gm$		7.16			
		Cooling		102.99	86.31	97.02	
		$\Delta H/J/gm$		5.32	7.16	55.14	
	TM	Cooling		103.5	87.2	72.79	
130.5	ABG	Cooling		89.1	81.8	50.70	
130.05	AB	Heating		104.59		73.4	
		$\Delta H/J/gm$		7.61		56.1	[10]
		Cooling		101.95	88.53	98.76	
		$\Delta H/J/gm$		7.88	4.44	59.82	
	TM	Cooling		103.5	89.4	74.30	
140.5	ABG	Cooling		89.3	83.7	51.74	
140.05	AB	Heating		104.43		76.2	[10]
		$\Delta H/J/gm$		14.99		58.0	
		Cooling		101.14	88.50	97.96	
		$\Delta H/J/gm$		14.63	9.21	103.80	
	TM	Cooling		104.5	91.3	75.78	
150.5	ABG	Cooling		86.4	84.0	92.16	
150.05	AB	Heating				78.4	
		$\Delta H/J/gm$				44.0	[10]
						100.33	
						112.34	

(Continued)

TABLE 2 Continued

Compound name	Phase variant	Method	Parameter	I-N/A/G	N/A-A/B/C	A-C/B	A/C-F/B	A/B/F-G	I/N/A/G-K	Ref.	
160.5 160.05		TM	Cooling	98.79	87.30				80.73	[10]	
			$\Delta H/J/gm$	13.21	5.50				87.74		
		TM		99.5	88.2				81.3		
	AF	TM	Cooling	84.0	81.8				62.8		
	A	DSC	Heating						96.91		
			$\Delta H/J/gm$						102.71		
180.5 180.05		TM	Cooling	90.18 ^a					89.48 ^a	[17]	
			$\Delta H/J/gm$						90.2		
		TM		91.3					56.6		
	F	TM	Cooling	83.7					91.57		
	Solid	DSC	Heating								119.83
			$\Delta H/J/gm$								81.45
			Cooling						111.10		
			$\Delta H/J/gm$						83.5		
			Cooling								

^aPeaks are not well resolved.

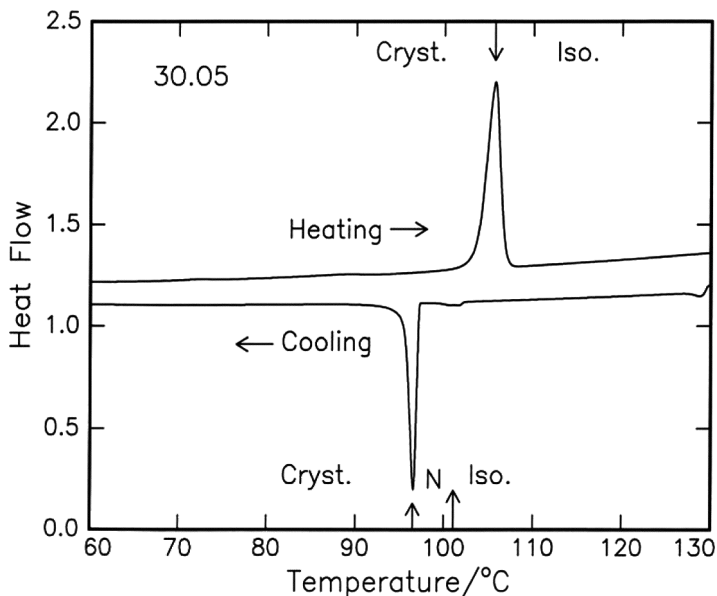


FIGURE 3 DSC heating and cooling thermogram of 30.05 compound.

phase transitions for $nO.05$ compounds. The DSC thermograms of 30.05, 70.05, 100.05, 130.05, and 160.05 are presented in Figs. 3–7.

Dilatometric Studies

The transition temperatures from dilatometric studies are found to agree with those obtained earlier from thermal microscopy and DSC measurements (Table 2). The slight temperature differences recorded from different techniques may be due the different scan rates. The phase-transition studies by density measurements are carried out across **IN**, **AK**, **NC**, **IA**, **AB**, and **CB** phase transitions in four members of $nO.05$ series: 70.05 (**NCBG**), 100.05 (**ABG**), 130.05 (**AB**), and 160.05 (**A**) and on 5.5 Nematic, Smectic G (**NG**) and 5.05 (**NG**).

The estimated molar volume (molecular weight/density) in isotropic phase per an increment of methylene unit estimated at $T_{(IN/IA)+5}$ is in the range of $15\text{--}16.5 \times 10^{-6} \text{ cm}^3 \cdot \text{mol}^{-1}$ and agrees with the body of the data available on $nO.m$ compounds and the values reported for normal liquids [7,12]. The temperature variation of density $\rho(T)$ and thermal expansion coefficient $\alpha(T)$ for the compounds ($n = 7, 10, 13,$ and 16) studied are shown in Figures 8–11. The trends

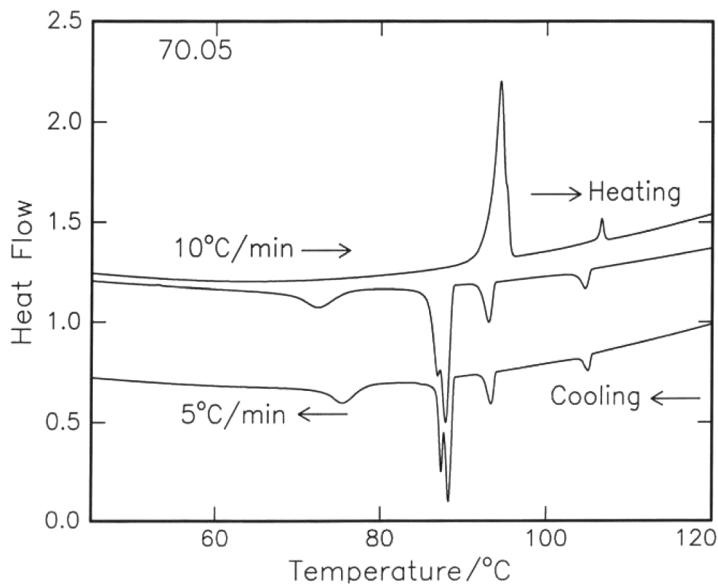


FIGURE 4 DSC heating and cooling thermograms of 70.05 compound at two different scan rates.

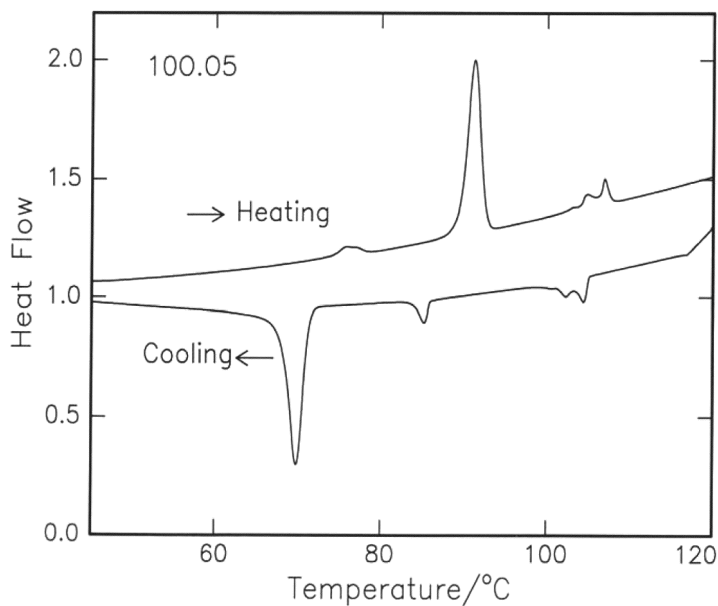


FIGURE 5 DSC heating and cooling thermogram of 100.05 compound.

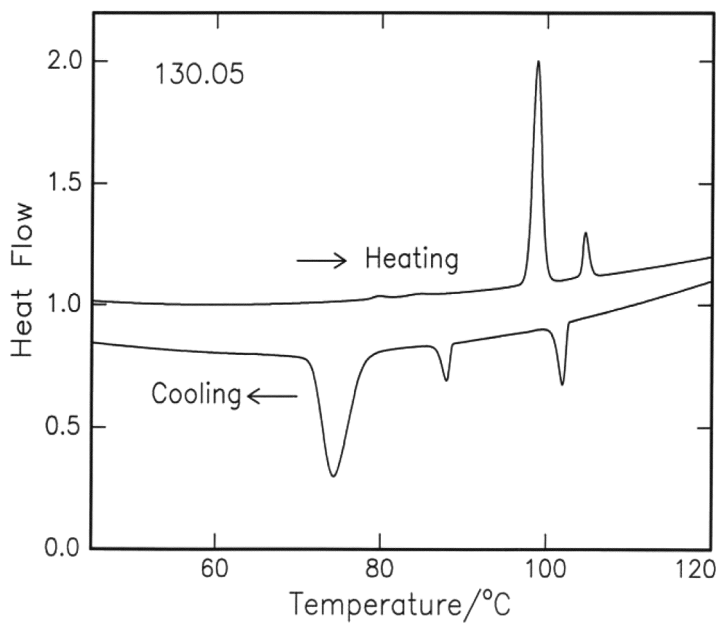


FIGURE 6 DSC heating and cooling thermograms of 130.O5 compound.

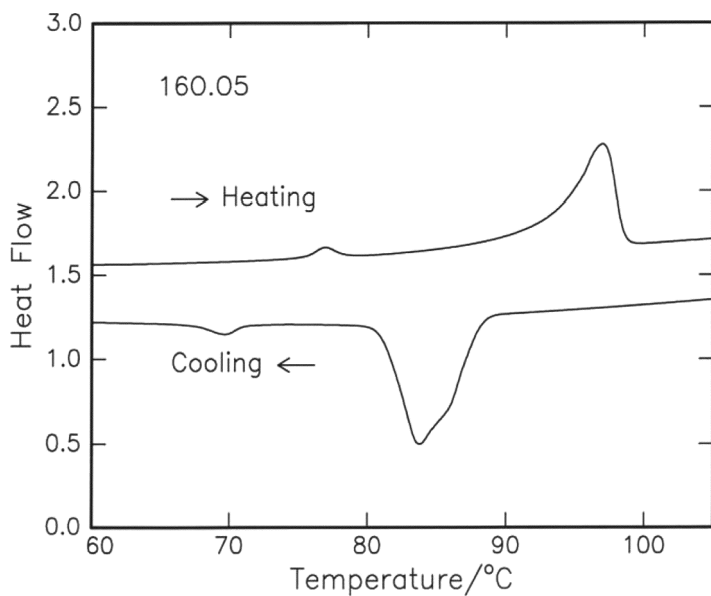


FIGURE 7 DSC heating and cooling thermograms of 160.O5 compound.

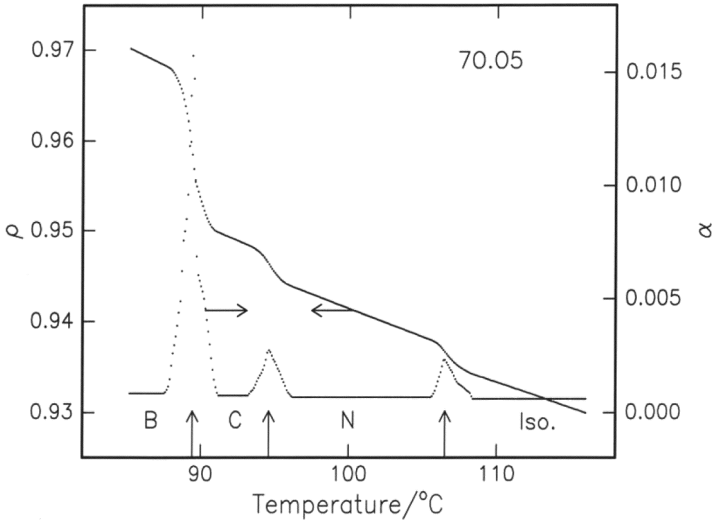


FIGURE 8 Temperature variation of density $\rho(T)$ and the thermal expansion coefficient $\alpha(T)$ of 70.05 compound.

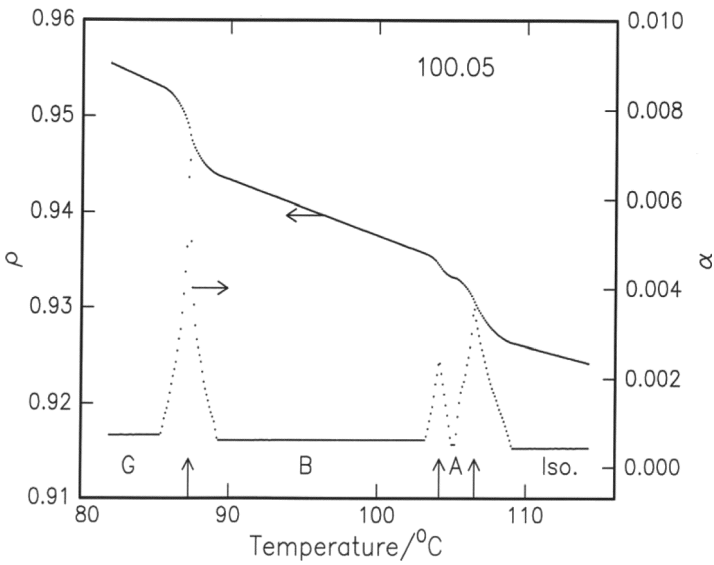


FIGURE 9 Temperature variation of density $\rho(T)$ and the thermal expansion coefficient $\alpha(T)$ of 100.05 compound.

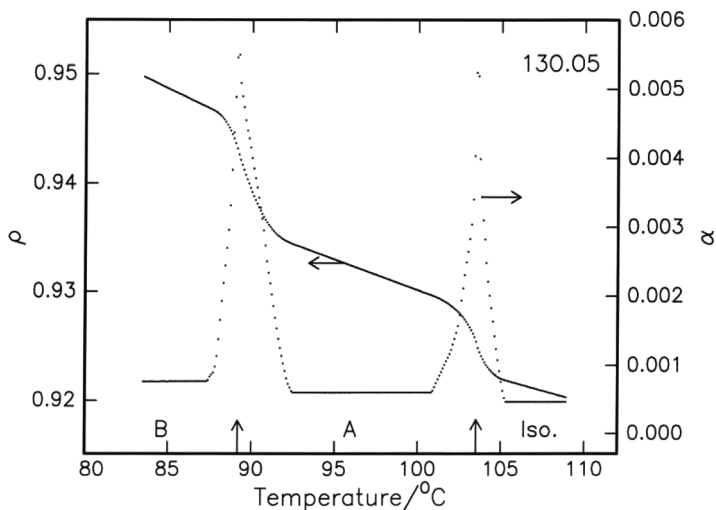


FIGURE 10 Temperature variation of density $\rho(T)$ and the thermal expansion coefficient $\alpha(T)$ of 130.05 compound.

of slopes in all LC phases are found to increase as one goes down from the isotropic to higher ordered LC phases. However, the values are relatively lower than those observed for $nO.m$ compounds in any LC

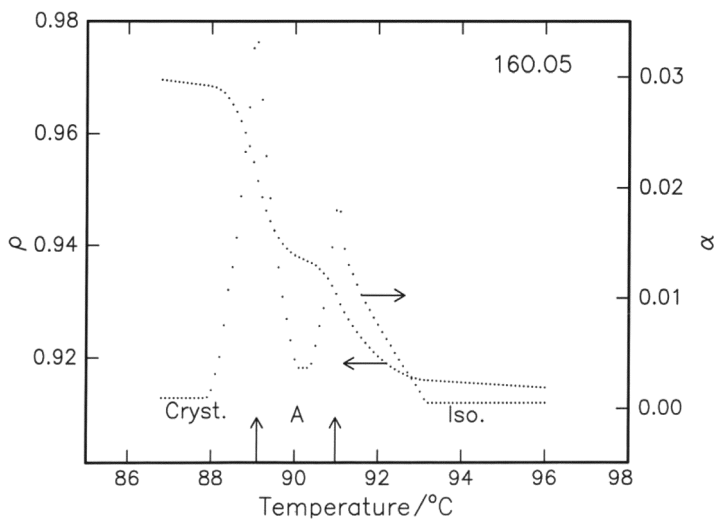


FIGURE 11 Temperature variation of density $\rho(T)$ and the thermal expansion coefficient $\alpha(T)$ of 160.05 compound.

TABLE 3 Slopes of Different Phases (the Magnitude Is Increasing from the Isotropic to Higher Ordered Liquid-Crystalline Phases)

Compound	Phase variant	Nematic/					Crystal	Ref.
		Isotropic	Smectic A	Smectic C	Smectic B	Smectic G		
70.O5	NCBG	5.7	6.4	7.2	8.3			PW
100.O5	ABG	4.2	18.6 ^a		6.0	7.2		PW
130.O5	AB	4.5	5.8		7.5			PW
160.O5	A	4.8	36.0 ^a				9.5	PW

^aThe thermal range of smectic A in these compounds is short, and hence the slope values are not reliable.

PW, Personal Work.

phase [7]. The slope values obtained for the compounds 70.O5, 100.O5, 130.O5, and 160.O5 are given in Table 3.

Isotropic to Nematic Transition (IN) in 70.O5

The density of this compound is found to increase with the decrease of temperature at I, N, S_C, and S_B phases in compound 70.O5 except in the vicinity of phase transitions. The vertical distance between the density values (ρ_1 and ρ_2) obtained by extrapolating the observed linear dependence to transition temperatures from either sides of the transition, when normalized over the average value of these two density values (i.e., $[(\rho_1 - \rho_2)/\{(\rho_1 + \rho_2)/2\}]$) is taken as the density jump ($\Delta\rho/\rho$) across the transition.

The observed density jump of 0.28% and the thermal expansion coefficient maxima of $23.5 \times 10^{-4} \text{ }^\circ\text{C}^{-1}$ (Fig. 8) indicate the IN transition to be first order. The density jump and thermal expansion coefficient maxima of these compounds along with the values for the some $nO.m$ compounds with equal chain lengths are given in Table 4. The

TABLE 4 Density Jump and Thermal Expansion Coefficient Maxima of 70.O5 Compound along with the Values of the Compounds with Equal Chain Lengths of Isotropic–Nematic Transition

Compound	Phase variant	% of ($\Delta\rho/\rho$)	$\alpha \times 10^{-4} \text{ }^\circ\text{C}^{-1}$	Ref.
70.O5	NCBG	0.28	23.5	PW
70.5	NACBG	0.34	103.6	[15]
50.7	NACBG	0.33	110	[18]
60.6	NABG	0.30	109	[19]
40.8		0.31	95	[20]

Note. The density jump is smaller compared to 70.5 and 50.7.

TABLE 5 Density Jump and Thermal Expansion Coefficient Values for Nematic–Smectic C Transition obtained for Compound 70.O5 vs. NOBA

Compound	Phase variant	% of ($\Delta\rho/\rho$)	$\alpha \times 10^{-4} \text{ }^\circ\text{C}^{-1}$	Ref.
70.O5	NCBG	0.28	23.5	PW
NOBA	NC	0.23	50	[13]

magnitude of density jump in all compounds is almost found to be same with total flexible identical chain length and exhibit IN transition.

Nematic to Smectic C Transition (NS_C) in 70.O5

A transition from an orientational ordered N phase to S_C phase possessing additional layered structure with a tilted order is expected to be the first order. The observed density jump ($\Delta\rho/\rho = 0.45$) and the thermal expansion coefficient maxima ($\alpha = 27.5 \times 10^{-4} \text{ }^\circ\text{C}^{-1}$) confirm the NS_C transition as first order. The data on $n\text{O}.m$ compounds reveal that no compound exhibits NS_C transition [1]. The values obtained for this compound are slightly lower to those obtained for NOBA [13] and are given in Table 5.

Isotropic to Smectic A Transition (IS_A) in 100.O5, 130.O5, and 160.O5

The IS_A transition in 100.O5, 130.O5, and 160.O5 is accompanied by a large density jump of 0.71%, 0.71%, and 2.10% and thermal expansion coefficient maxima of $35.4 \times 10^{-4} \text{ }^\circ\text{C}^{-1}$, $52.3 \times 10^{-4} \text{ }^\circ\text{C}^{-1}$, and $180.0 \times 10^{-4} \text{ }^\circ\text{C}^{-1}$ respectively indicate the transition is of first-order nature. The density jumps and thermal expansion coefficient maxima of the present $n\text{O}.05$ compounds along with the other in $n\text{O}.m$ compounds that exhibit IS_A transition are presented in Table 6.

It is noticed that the density jumps obtained in the compounds 100.O5 and 130.O5 are slightly less than those found in the case of $n\text{O}.m$ compounds, whereas the value of $\Delta\rho$ in the compound 160.O5 is found to be highest reported for benzylidene anilines ($n\text{O}.m$) compounds (exhibiting a single phase variant, S_A) [14]. The dilatometric studies across IS_A transition are accompanied by large thermal span of fluctuation-dominated nonlinear regions (FDNLR) to an extent of $\sim 2.0^\circ\text{C}$ in these three compounds. The growth of S_A phase is observed as a pyknometer as the translucent S_A phase grows at the bottom of the bulb, while transparent isotropic liquid floats over it. The S_A phase with a clear separation boundary is found to spread gradually from the

TABLE 6 Density Jumps and Thermal Expansion Coefficient Maxima of These Compounds along with the Other Compounds in Benzylidene Aniline Series that Exhibit Isotropic–Smectic A (IS_A) Transition

Compound	Phase variant	% of $(\Delta\rho/\rho)$	$\alpha \times 10^{-4} \text{ } ^\circ\text{C}^{-1}$	Ref.
100.O5	ABG	0.71	35.4	PW
130.O5	AB	0.71	52.3	PW
160.O5	A	2.10	180.0	PW
70.8	ACBG	1.04	225.0	[21]
80.7	ACBG	1.32	146.0	[22]
90.6	ACFG	1.51	440.0	[22]
140.1	A	0.93	133.7	[23]
80.10	ABF	0.90	239.0	[15]
100.8	ACFG	1.50	629.0	[12]
70.14	ABG	0.99	124.0	[24]
90.12	ABG	0.90	123.0	[7]

isotropic liquid all through the pycnometer with the decrease of temperature. The formation of S_A embryos at the bottom of the bulb and their consequential growth clearly indicates the nucleation type of growth at IS_A phase transition. The visual observation of translucent S_A phase, which is clearly distinct from milky or cloud = like appearance in the entire bulb of nematic phase, suggests the simultaneous onset of orientational and translational orders rather than preferential growth of one over the other.

Smectic A to Smectic B ($S_A S_B$) Transition in 100.O5 and 130.O5

The $S_A S_B$ transition is associated with the development of long-range three-dimensional order and molecular correlation of hexagonal in-plane stacking with its layered structure. The observed density jumps ($\Delta\rho/\rho$) of 0.25 and 1.18 and thermal expansion coefficient maxima (α_{\max}) of $23.5 \times 10^{-4} \text{ } ^\circ\text{C}^{-1}$ and $54.8 \times 10^{-4} \text{ } ^\circ\text{C}^{-1}$ for the 100.O5 and 130.O5 respectively indicate the first-order nature of transition. The large variation of density jump values in the case of these two compounds is not an uncommon trend as observed in the case some $nO.m$ compounds (80. m series) [15]. The density jumps and thermal expansion coefficient maxima for these compounds along with the other compounds are presented in Table 7. However, the sticky nature of substance (to the inner walls of the pycnometer) did not permit further investigation of $\rho(T)$ deep into the S_B phase as well as the $S_B S_G$ phase transition in the 100.O5 compound because the compound develops breaks in the pycnometer columns.

TABLE 7 Density Jumps and Thermal Expansion Coefficient Maxima obtained for Smectic A–Smectic B Transition along with the Comparison of $nO.m$ Compounds

Compound	Phase variant	% of $(\Delta\rho/\rho)$	$\alpha \times 10^{-4} \text{ }^\circ\text{C}^{-1}$	Ref.
100.O5	ABG	0.25	23.5	PW
130.O5	AB	1.18	54.8	PW
70.10	AB	1.37	357	[11]
70.14	ABG	0.99	124.0	[24]
80.4	ABG	0.40	85.0	[25]
80.5	ABG	0.54	92.0	[11]
80.8	ABG	0.24	71.0	[21]
80.9	ABG	0.60	60.0	[11]
80.10	ABF	1.41	376.0	[15]
80.14	ABG	1.10	154.0	[24]
90.12	ABG	0.68	107.0	[7]
90.14	ABG	1.60	156.0	[24]
90.16	ABG	0.74	112.0	[7]

Smectic C to Smectic B ($S_C S_B$) Transition in 70.O5

The S_C phase is the tilted analogue of S_A phase. The smectic layers possess a liquid-like unstructured arrangement of a lath-like molecules that are tilted with respect to the layer planes at angles, which vary from compound to compound. Further, for a given compound, the tilt angle may either vary or stay relatively constant with temperature over the thermal range of S_C phase. The S_B phase that forms from the S_C phase on cooling regains the orthogonal alignment of the molecules in addition to the long-range order within the smectic layer planes. The S_B phase possesses long-range three-dimensional (3D) order and positional correlations of the hexagonal in-plane packing of the molecules as well as the layer stacking. Hence, the transition from S_C to S_B phase is expected to be first order. The observed large density jump $(\Delta\rho/\rho)$ of 1.76% and the thermal coefficient maxima $\alpha_{\max.}$ of $157.2 \times 10^{-4} \text{ }^\circ\text{C}^{-1}$ (Table 8) confirm the order of the transition to be first order in the compound 70.O5. The density variation across the $S_C S_B$ transition does not, however, correspond to a step function. Instead, it exhibits an almost linear behavior with a finite slope. The values of density jumps across this transition are generally found to be less than at the $S_A S_B$ transition. As the structural environment on the higher temperature side $S_A S_B$ transition is much less ordered (in comparison to that across $S_C S_B$ transition), a lower jump in the latter case is justifiable. For reference, the observed density jumps in other $nO.m$ compounds, which exhibit the same transition, are given in Table 8.

TABLE 8 Observed Density Jumps and Thermal Expansion Coefficients for Smectic C–smectic B Transition of 7O.05 Compound along with the $nO.m$ Compounds that Exhibit the Same Transition

Compound	Phase variant	% of $(\Delta\rho/\rho)$	$\alpha \times 10^{-4} \text{ } ^\circ\text{C}^{-1}$	Ref.
7O.05	NCBG	0.28	23.5	PW
7O.5	NACBG	0.76	163.0	[10]
5O.7	NACBG	0.50	108.0	[18]
4O.7	NACB	0.41	267.0	[26]
7O.7	NCB	0.93	249.0	[19]
7O.8	ACBG	0.84	92.0	[21]
8O.6	ACBG	0.79	101.0	[11]
8O.7	ACBG	0.79	107.0	[11]
10O.9	ACBG	1.27	381.0	[12]

Smectic A to Crystalline Solid (S_{AK}) in 16O.05

This transition involving a change from long-range orientational order with layered arrangement to a perfectly three-dimensional crystal is expected to first order. However, the dilatometric investigation, as in the case of 16O.05, showed the transition temperature involved is high compared to those compounds that exhibit this transition in $nO.m$ compounds. Further, the thermal range of S_A phase in 16O.05 is found to be as low as 1.9°C . The observed density jump $(\Delta\rho/\rho)$ of 3.0% and the thermal coefficient maxima α_{max} of $330.8 \times 10^{-4} \text{ } ^\circ\text{C}^{-1}$ at this transition confirm the order of transition as first order in the compound 16O.05. Further, the observed largest density jump across the $S_A S_K$ transition implies the lower phase as nearer to the perfect solid phase. For comparison, the transition temperature involved and the thermal range of S_A phase exhibited by different compounds in $nO.m$ series are presented in Table 9.

Pretransitional Effects Across Isotropic to First LC Phase

The observed nonlinear density variation on the isotropic side (fluctuation dominated nonlinear regions, FDNLR) represents the varied volume swept by the molecules (with characteristic hindered rotational degrees of freedom). As such these fluctuations are accompanied by the density variation, which grows during the condensation of the low-temperature LC phase. In the vicinity of the phase transformation, the volume occupied by the molecules with a specified potential energy is influenced by the growth of low-temperature mesophase with a specific molecular structure. Further, the FDNLR on both sides

TABLE 9 Transition Temperature Involved and the Thermal Range of S_A for Different Compounds in *nO.m* Series

Compound	Transition temperature (°C)	Thermal range of S _A phase (°C)	Ref.
16O.05	91.0	1.9	PW
2O.16	70.1	17.9	[27]
13O.1	76.3	15.3	[28]
14O.1	76.5	7.9	[16]

of the interface depends on the LC phase (on the low-temperature side of the transition). The growth of a LC phase through the underlying density fluctuation from isotropic liquid is estimated by an exponent α by fitting the observed density data [in FDNLR for $T > T_C$] to the following relation

$$|\rho_I - \rho_c| \alpha |T_I - T_c|^{(1-\alpha_{\text{eff}})}, \quad (1)$$

where ρ_i is the observed density at temperature of interest T_i and ρ_c is the observed density at isotropic to LC transition (i.e., $T_{I-N/A}$). As $\Delta T = |T_i - T_c|$ reflects the thermal range of pretransition of fluctuation in the FDNLR, they imply the longevity of the fluctuations. However, α_{eff} reflects the strength of the fluctuations.

The observed temperature variation data of density $\rho(T)$ and transition temperatures T_c are fitted to the relation (1), and the resulting α_{eff} values and the data of thermal span of FDNLR are listed in Table 10 along with the data of some *nO.m* compounds. The goodness

TABLE 10 Resulting α_{eff} Values along with the Data of Thermal Span of FDNLR along with the Data on Some *nO.m* compounds

Compound	Transition	α_{eff}	FDNLR (°C)	Ref.
7O.05	IN	0.20	2.0	PW
7O.5	IN	0.57	0.4	[15]
6O.6	IN	0.26	0.4	[19]
4O.8	IN	0.79	0.4	[20]
10O.05	IA	0.26	2.5	PW
9O.6	IA	0.62	1.3	[22]
8O.7	IA	0.18	1.4	[15]
7O.8	IA	0.45	0.5	[21]
13O.05	IA	0.38	1.9	PW
10O.8	IA	0.63	1.2	[12]
16O.05	IA	0.35	2.2	PW
7O.14	IA	0.62	1.4	[24]

of the fit is demonstrated through the p values (> 0.996) corresponding to the χ^2 test in the present compounds.

CONCLUSION

It may, therefore, be concluded from this discussion that the placement of an oxygen atom plays an important role in forecasting the polymorphism, and the alkyl chain length further tunes the occurrence of phase variant in benzylidene aniline compounds. Further, the oxygen atom on both sides of the rigid core moiety has no major effect on the order of transition in comparison with *nO.m* compounds.

ACKNOWLEDGMENT

The financial support of the Department of Science and Technology (Grant No. SP/S2/M-34/2000), New Delhi, India, is gratefully acknowledged.

REFERENCES

- [1] Pisipati, V. G. K. M. (2003). *Z. Naturforsch.*, 58(a), 661–663.
- [2] Smith, G. W., Gardlund, Z. G., & Curtis, R. J. (1973). *Mol. Cryst. Liq. Cryst.*, 19, 327–330.
- [3] Ajeetha, N. & Pisipati, V. G. K. M. (2003). *Z. Naturforsch.*, 58(a), 735–737.
- [4] Ajeetha, N., Potukuchi, D.M., & Pisipati, V. G. K. M. (2004). *Phase Trans.*, 78, 369–375.
- [5] Galewski, Z., Sienkowska, M., & Hoffmanska, A. (2002). *Proc. SPIE-Int. Soc. Opt. Eng.*, 4759, 85–89.
- [6] Cruz, C., Heinrich, B., Riberiro, A. C., Bruce, D. W., & Guillon, D. (2000). *Liq. Cryst.*, 27, 1625–1631.
- [7] Prabu, C. R. C., Lakshminarayana, S., & Pisipati, V. G. K. M. (2004). *Z. Naturforsch.*, 59(a), 537–542.
- [8] Smith, G. W., & Gradlund, Z. G. (1973). *J. Chem. Phys.*, 59, 3214–3228.
- [9] Rao, N. V. S., Pisipati, V. G. K. M., Prasad, P. V. D., Alapati, P. R., Potukuchi, D. M., & Petrov, A. G. (1989). *Bul. J. Phys.*, 16, 93–104.
- [10] Padmaja, S., Srinivasulu, M., & Pisipati, V. G. K. M. (2003). *Z. Naturforsch.*, 58(a), 573–580.
- [11] Prabu, C. R. C., & Pisipati, V. G. K. M. (2002). *Cryst. Res. Technol.*, 37, 269–280.
- [12] Prabu, C. R. C. (1998). Ph. D. Thesis, “Phase transitions in liquid crystalline benzylidene anilines—a dilatometric study,” Nagarjuna University, India.
- [13] Rao, N. V. S., & Pisipati, V. G. K. M. (1985). *Z. Naturforsch.*, 40(a), 466–468.
- [14] Pisipati, V. G. K. M., Rao, N. V. S., Reddy, M. V. V. N., Rao, C. G. R., & Padmavathi, G. (1991). *Cryst. Res. Technol.*, 26, 709–716.
- [15] Rao, N. V. S., Pisipati, V. G. K. M., Sankar, Y. G., & Potukuchi, D. M. (1986). *Phase Trans.*, 7, 49–58.
- [16] Rao, P. B., Rao, N. V. S., Pisipati, V. G. K. M., & Saran, D. (1986). *Cryst. Res. Technol.*, 24, 723–731.

- [17] Jitendranadh, M., Rao, C. G. R., Srinivasulu, M., & Pisipati, V. G. K. M. (2001). *Mol. Cryst. Liq. Cryst.*, 366, 47–59.
- [18] Pisipati, V. G. K. M., George, A. K., Srinivasu, C., & Murthy, P. N. (2003). *Z. Naturforsch.*, 58a, 103–108.
- [19] Alapati, P. R., Potukuchi, D. M., Rao, N. V. S., Pisipati, V. G. K. M., Prajape, A. S., & Rao, U. R. K. (1988). *Liq. Cryst.*, 3, 1461–1479.
- [20] Rao, P. B., Potukuchi, D. M., Murthy, J. S. R., Rao, N. V. S., & Pisipati, V. G. K. M. (1992). *Cryst. Res. Technol.*, 27, 839–849.
- [21] Rao, N. V. S., Potukuchi, D. M., & Pisipati, V. G. K. M. (1991). *Mol. Cryst. Liq. Cryst.*, 196, 71–87.
- [22] Pisipati, V. G. K. M., Murthy, J. S. R., Rao, N. V. S., & Sankar, Y. G. (1986). *Acustica*, 60, 163–168.
- [23] Rao, N. V. S., Potukuchi, D. M., Rao, P. V. S., & Pisipati, V. G. K. M. (1992). *Liq. Cryst.*, 12, 127–135.
- [24] Baskaran, G. S. (2004). M. Phil. Thesis, “Synthesis, characterization and phase transition studies across isotropic to smectic A phase in a mesomorphic N (p-n-tetradecyloxybenzylidene) p-n-toluidine, 14O.1,” Nagarjuna University, India.
- [25] Jitendranadh, M., Rao, C. G. R., Srinivasulu, M., Potukuchi, D. M., & Pisipati, V. G. K. M. (2001). *Mol. Cryst. Liq. Cryst.*, 366, 457–471.
- [26] Pisiapti, V. G. K. M., & Rao, N. V. S. (1983). *Phase Trans.*, 3, 169–176.
- [27] Rao, N. V. S., Potukuchi, D. M., & Pisipati, V. G. K. M. (1991). *Mol. Cryst. Liq. Cryst.*, 196, 71–87.
- [28] Kumar, P. A., Madhu Mohan, M. L. N., & Pisipati, V. G. K. M. (2000). *Liq. Cryst.*, 27, 727–735.
- [29] Rao, M. R. K., M. Phil. Thesis, “Synthesis, characterization and dilatometric study on mesomorphic N(p-n-tridecyloxybenzylidene) p-n-toluidine, 13O.1,” Nagarjuna University, India (2003).